Synthesis, Self-Assembly, and Magnetic Properties of $[FePt]_{1-x}Au_x$ Nanoparticles

Shishou Kang, Zhiyong Jia, David E. Nikles, and J. W. Harrell, *Member, IEEE*

***Abstract*—$[FePt]_{1-x}Au_x$ nanoparticles were prepared by the simultaneous polyol reduction of platinum acetylacetonate and gold acetate and the thermal decomposition of iron pentacarbonyl, giving 3.5-nm-diameter FePt particles with gold atoms substituted in the lattices. The addition of gold promoted the face-centered cubic to tetragonal phase transition, thereby reducing the temperature required for this transition by more than 150 °C compared with FePt nanoparticles with no additives. This effect is even more significant than adding silver to FePt nanoparticles. For a given annealing temperature, the coercivity increases with the content of gold up to 24%, above which the coercivity starts to decrease. The mechanism for the chemical ordering acceleration may relate to the defect and strains introduced by gold atoms. Upon annealing, gold atoms leave the FePt lattice, leaving lattice vacancies that increase the mobility of the FePt atoms to rearrangement. Dynamic coercivity measurements yield thermal stability factors that are slightly higher than would be expected for noninteracting particles.**

***Index Terms*—FePt, hard magnet materials, high K_u alloys, $L1_0$ phase, magnetic recording, nanoparticle synthesis, self-assembly.**

I. Introduction

MAGNETIC recording technology has made tremendous gains in data storage density, partly by scaling down the grain size of thin-film media. However, further scaling to support future increases will bring the grain sizes near the superparamagnetic limit. This has led to a search for new materials and new microstructures for magnetic recording. The FePt-base nanostructured materials are excellent candidates because of their good chemical stability and high magnetocrystalline anisotropy ($\sim 7 \times 10^7$ erg/cc) observed in the ordered intermetallic phase [1], [2]. This large crystalline anisotropy allows for thermally stable grain diameters down to 2.8 nm. The synthesis and characterization of a well-organized magnetic array of such particles can contribute to the design of a magnetic medium capable of recording densities beyond 1 Tb/in^2 [3], [4]. The challenges to realize this Tb/in^2 goal are to make uniform high-coercivity FePt nanoparticles and nanoparticle assemblies with controlled assembly thickness, surface roughness, and mechanical robustness. Various vacuum deposition techniques have been developed to make high-coercivity FePt nanocrystalline films [5]–[9]. Post-annealing was necessary to transform the as-made chemically disordered fcc structure into the chemically ordered face-centered tetragonal (fct) structure that has high magnetocrystalline anisotropy. Random nucleation in the initial stages of the growth, however, typically results in broad distributions of particle sizes, which may be further aggravated by agglomeration during annealing [10]–[13].

A recent report by Sun *et al.* has generated considerable interest in the use of self-assembled FePt nanoparticles for ultrahigh-density recording media [14]. As-prepared FePt nanoparticles have a face-centered cubic (fcc) structure and are superparamagnetic. The particles are coated with organic surfactants (oleic acid and oleylamine) and can be dispersed in hydrocarbon solvents. When the dispersions are cast onto solid substrates and the solvent evaporates, the particles self-assemble into close-packed arrays. After heat treatment at high temperature ($\geq$550 °C), the particles transform to the tetragonal phase, having high magnetocrystalline anisotropy and giving films with high coercivity. However, these high temperatures would be undesirable for processing of media. Recently we have reported on the effect of additive silver in promoting the chemical ordering of self-assembled FePt nanoparticles [15]. In this paper, we report the synthesis of self-assembled $[FePt]_{1-x}Au_x$ nanoparticles and the even greater beneficial effect of the added gold on the phase transformation.

II. Experimental Procedures

A. Synthesis of $[FePt]_{1-x}Au_x$ Nanoparticles

The nanoparticles were prepared using a modification of the procedure reported by Sun *et al.* [14]. The synthetic experiments were carried out using standard airless procedures and commercially available reagents. A solution of platinum acetylacetonate (0.5 mmol), gold acetate (0.05–0.35 mmol), and 1,2-hexadecanediol (1.5 mmol) in 20-mL phenyl ether was heated to 80 °C in a three-necked round-bottom flask under a nitrogen atmosphere. To this solution was added via syringe oleic acid (0.5 mmol), oleylamine (0.5 mmol), and iron pentacarbonyl (1 mmol). The mixture was heated to reflux and allowed to reflux for 30 min giving a black dispersion. The heat source was then removed and the dispersion was allowed to cool to room temperature. The inert gas protected system could then be opened to ambient environment. The black product was precipitated by adding 40-mL ethanol.

Manuscript received January 6, 2003. This work was supported by the National Science Foundation Materials Research Science and Engineering Center (MRSEC) Program under Award DMR-0213985.

S. Kang is with the Center for Materials for Information Technology, The University of Alabama, Tuscaloosa, AL 35487-0209 USA (e-mail: skang@mint.ua.edu).

Z. Jia and J. W. Harrell are with the Department of Physics and Astronomy and the Center for Materials for Information Technology, The University of Alabama, Tuscaloosa, AL 35487-0324 USA (e-mail: jia002@bama.ua.edu; jharrell@bama.ua.edu).

D. E. Nikles is with the Department of Chemistry and the Center for Materials for Information Technology, The University of Alabama, Tuscaloosa, AL 35487-0336 USA (e-mail: dnikles@mint.ua.edu).

Digital Object Identifier 10.1109/TMAG.2003.815589

The mixture was centrifuged to isolate the particles from the brown supernatant. The particles were redispersed in hexane, precipitated with ethanol, and isolated by centrifuging. The particles were dried at room temperature in a vacuum oven to give 100–200 mg of particles. The dispersion and precipitation removed impurities. The contents of the supernatant solution were not analyzed. During synthesis, the relative mounts of platinum acetylacetonate and iron pentacarbonyl were fixed. The amount of gold acetate was varied in order to produce nanoparticles with different compositions.

B. Structural Characterization and Magnetic Measurements of $[FePt]_{1-x}Au_x$ Nanoparticle Assemblies

The particles were dispersed in a 50/50 mixture of hexane and octane (10-mg particles in 1-mL solvent), containing 0.1 mL of a 50/50 mixture of oleylamine and oleic acid. The dispersion was dropped onto a solid substrate and the solvent was allowed to evaporate slowly at room temperature. Using octane in the solvent mixture slowed the solvent evaporate rate relative to pure hexane. The as-made thin films were then transferred into a Lindberg tube furnace for thermal annealing. The annealing temperature ranged from 300 °C to 500 °C. During annealing, Ar with 5% hydrogen was flowing through the furnace. The temperature was elevated at a rate of 40 °C/min and was then kept at the desired temperature for 30 min.

Fe, Pt, and Au elemental analyses of as-synthesized $[FePt]_{1-x}Au_x$ were performed with energy-dispersive X-ray analysis on a Philips model XL 30 scanning electron microscope. A thin FePt nanoparticle assembly was made by spreading dilute particle dispersion onto a carbon-coated copper TEM grid (200 mesh from SPI) and analyzed using a Hitachi HF-2000 TEM in order to determine the particle size and microstructure. The nanoparticle structure was characterized in the reflection geometry with a Rigaku powder diffractometer using CuK_α radiation.

Magnetic studies were carried out using a Princeton Measurements Model 2900 alternating gradient magnetometer (AGM) with maximum applied field of 19 kOe and an Oxford Instruments vibrating sample magnetometer (VSM) magnetometer with field up to 9 T and temperature from 10 to 300 K. All measurements were made with the applied magnetic field in the plane of the films.

III. Results and Discussion

A. Formation of $[FePt]_{1-x}Au_x$ Nanoparticle Assemblies

When the FePtAu nanoparticle dispersions are spread onto a substrate and the carrier solvent is allowed to slowly evaporate, FePtAu nanoparticle superlattices are produced. For TEM observation, a drop ($\sim$0.5 μL) of a dilute $[FePt]_{1-x}Au_x$ dispersion ($\sim$1 mg/mL) was deposited on a carbon-coated copper grid. TEM images for the films (Figs. 1 and 2) showed that the particle assembled into hexagonal arrays. In thin regions of the films (Fig. 1), the particles formed a honeycomb array consistent with AB stacking of the particles, while in thicker regions of the films (Fig. 2) the particles assembled into an ABC close-packed structure. The average particle size was 3.5 nm. The space between the particles was occupied by the surfactants, oleic acid, and oleylamine. In a previous study, Rutherford backscattering measurements on annealed FePt samples revealed that annealing at high temperature does not result in the loss of these surfactants; rather, they are converted to a carbonaceous coating around each particle, effectively protecting particles from agglomeration [14].

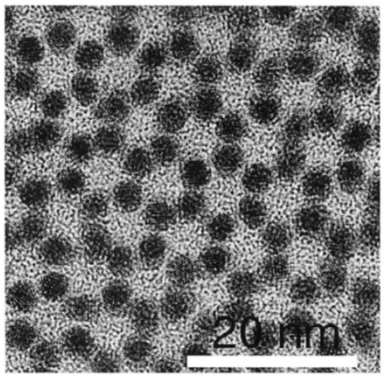

Fig. 1. TEM image of a thin film consisting of as-made $[FePt]_{85}Au_{15}$ nanoparticles.

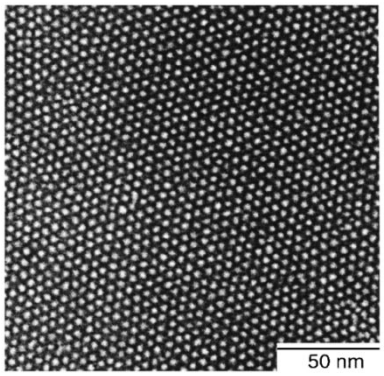

Fig. 2. TEM image of a thick film consisting of as-made $[FePt]_{92}Au_8$ nanoparticles.

B. $[FePt]_{1-x}Au_x$ Nanoparticle Structure

Fig. 3 illustrates the XRD patterns of as-made $[FePt]_{1-x}Au_x$ nanoparticles. The as-made particles show a typical chemically disordered fcc structure with three-dimensional (3-D) random orientation. With increasing gold content, the (111) peak of $[FePt]_{1-x}Au_x$ nanoparticles shift to the low angle, which means the lattice of the FePt nanoparticles was expanded after introducing gold, indicating that gold was substituting into the FePt lattice.

Annealing induces the Fe and Pt atoms to rearrange into the long-range chemically ordered fct phase. The change of the internal particle structure upon annealing depends on annealing temperature, as well as the content of gold. The sequence of X-ray diffraction (XRD) curves in Fig. 4(a) and (b) illustrates the development of the chemically ordered $L1_0$ phase of FePt nanoparticles as a function of annealing temperature for samples with addition of 8% and 15% gold, respectively. The phase transformation can be seen by the evolution of the (001) and (110) peaks, and the shift of the (111) peaks to high angle with increasing annealing temperature. Furthermore, we can clearly see the splitting of (200) and (002) peaks due to the fct struc-

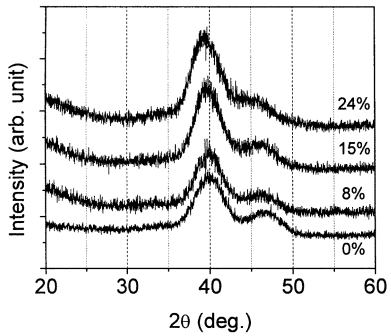

Fig. 3. XRD patterns for as-prepared $[FePt]_{1-x}Au_x$ nanoparticles with $x = 0\%$, 8%, 15%, and 24%.

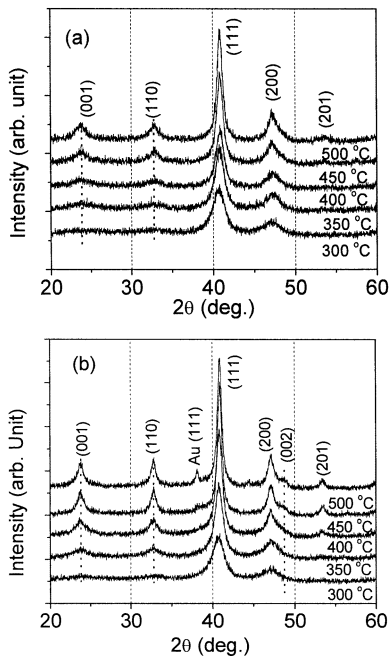

Fig. 4. XRD patterns for annealed $[FePt]_{1-x}Au_x$ nanoparticles with: (a) $x = 8\%$ and (b) $x = 15\%$.

ture of the samples with increasing annealing temperature in Fig. 4(b). Careful examination of the curves in Fig. 4(a) and (b) shows that very weak (001) and (110) peaks for the tetragonal FePt phase appeared after heat treatment at 300 °C, indicating that partial ordering begins around this temperature. This temperature, however, is more than 150 °C below that required for self-assembled FePt nanoparticles with no additive [14]. In Fig. 4(b), a shoulder appears at the low 2θ side of the FePt (111) peak, indicating that gold phase separates from the particles. The lack of the Au (111) peak in Fig. 4(a) may be due to the low content of Au in the particles.

The plots in Fig. 5 compare values of the (111) lattice spacing for $[FePt]_{1-x}Au_x$ nanoparticles as a function of annealing temperature. The (111) lattice spacing approaches the bulk value for tetragonal FePt ($d_{111} = 2.197$ Å) at a lower annealing temperature after introducing gold, indicating the phase transition was promoted by the addition of gold.

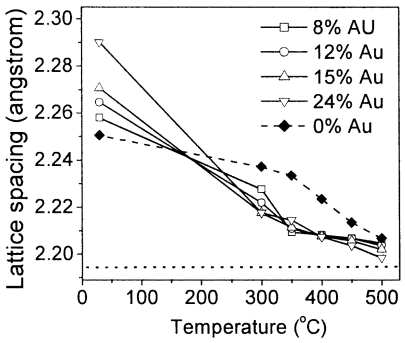

Fig. 5. Plot of d spacing for the (111) diffraction peak as a function of annealing temperature for $[FePt]_{1-x}Au_x$ nanoparticles with $x = 0\%$, 8%, 12%, 15%, and 24%. The dotted line indicates the bulk value of the d_{111} spacing of tetragonal FePt.

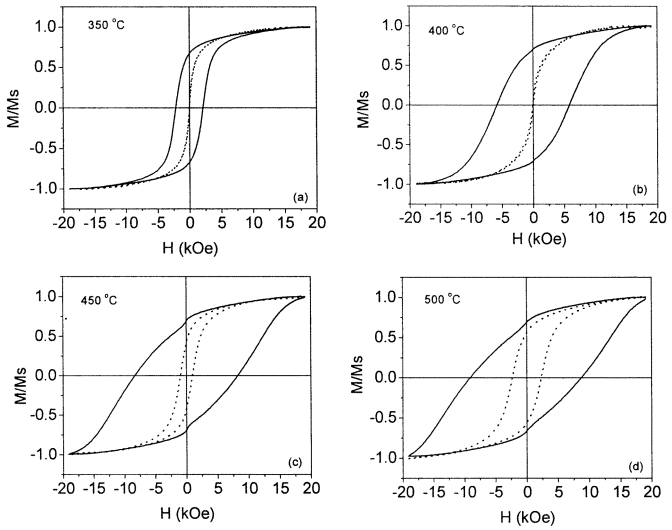

Fig. 6. Room-temperature hysteresis loops of $[FePt]_{85}Au_{15}$ (solid line) and pure FePt (dashed line) nanoparticles annealed at (a) 350 °C, (b) 400 °C, (c) 450 °C, and (d) 500 °C.

C. Magnetic Properties of $[FePt]_{1-x}Au_x$ Nanoparticles

The role of the annealing temperature on the chemical ordering and magnetic properties was probed using magnetometry. AGM measurements on as-made $[FePt]_{1-x}Au_x$ nanoparticles show that they are superparamagnetic at room temperature. After heat treatment, the particles partially transform to the fct structure with sufficient anisotropy to be ferromagnetic at room temperature. Shown in Fig. 6 are the room-temperature hysteresis loops for FePt nanoparticles with 15% gold annealed at 350 °C, 400 °C, 450 °C, and 500 °C for 30 min. For comparison, the loops of pure self-assembled FePt nanoparticles annealed under the same conditions are also plotted. For samples with additive gold, the coercivity increases dramatically with annealing temperature. With the annealing temperature up to 400 °C, the film containing FePt nanoparticles with no gold was still superparamagnetic, while the film containing FePt nanoparticles with 15% gold was ferromagnetic with an apparent coercivity greater than 5 kOe. The actual value exceeds this value because the maximum field on the AGM was not sufficient to completely saturate the film. It is obvious that the coercivity of the FePt nanoparticles was enhanced with the addition of Au.

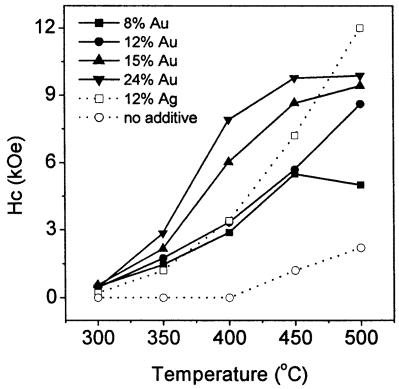

Fig. 7. Annealing temperature dependence of coercivity of $[FePt]_{1-x}Au_x$ nanoparticles with $x = 0\%$, 8%, 12%, 15%, and 24%. For comparison, the coercivity of $[FePt]_{88}Ag_{12}$ [15] as a function of the annealing temperature was also plotted.

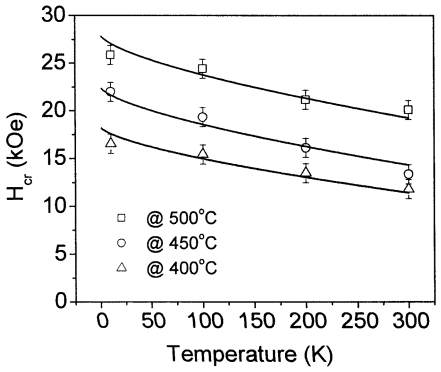

Fig. 8. Temperature-dependent H_{cr} of $[FePt]_{76}Au_{24}$ nanoparticles annealed at different temperature. The solid symbols are the measured values and the lines are the fits.

Fig. 7 shows the dependence of coercivity on the annealing temperature for FePt nanoparticles containing 8%, 12%, 15%, and 24% gold. For comparison, the coercivity of pure self-assembled FePt nanoparticles and FePt nanoparticles with an optimum silver composition of 12% annealed under the same conditions is also plotted [15]. For $[FePt]_{1-x}Au_x$ nanoparticles, the coercivity depends on the annealing temperature, as well as the concentration of gold. In general, the coercivity increases with the content of gold up to 24%. When the concentration of gold is increased further, the coercivity starts to decrease. Although both Au and Ag can significantly enhance the coercivity, a comparison of the coercivity of $[FePt]_{1-x}Au_x$, $[FePt]_{88}$ Ag_{12} (optimum composition), and FePt nanoparticles shows that gold has an even greater beneficial effect than silver in reducing the ordering temperature necessary for high Hc.

As mentioned above, the lattice of FePt nanoparticles with Au additive was expanded because the atomic volume of Au is larger than that of Fe and Pt. Thus, the elastic energy of the FePt system increased. On the other hand, Au has a low surface energy and is easy to segregate [16]. It appears that the Au atoms leave the FePt lattice at low temperature, leaving lattice vacancies. These vacancies, together with increased elastic energy of the FePt system, increase the mobility of the FePt atoms to rearrangement and, as a result, the kinetics of the ordering process is enhanced, the chemical ordering is accelerated, and the coercivity increases.

Fig. 8 shows the temperature dependence of the remanent coercivity H_{cr} for FePt nanoparticles with 24% gold annealed at 400 °C, 450 °C, and 500 °C measured with the Oxford VSM. In all cases, H_{cr} monotonically decreases with increasing temperature. The thermal stability factors KV/kT and intrinsic coercivities H_0 can be evaluated by fitting the following equation [17]:

$$H_{cr} = H_0 \cdot \left(1 - \left(\frac{kT}{KV} \cdot \ln\left(\frac{t \cdot f_0}{\ln 2}\right)\right)^{2/3}\right)$$

where k is the Boltzman's constant, K is the magnetic anisotropy energy, t is the waiting time of applied field ($\sim$1 s), f_0 is the attempt frequency ($\sim 10^9$ Hz), and V is the magnetic switching volume. Assuming KV is a constant with the temperature, the fits of data in Fig. 8 yield H_0 values of 18, 23, and 28 kOe. At room temperature, the thermal stability factors KV/kT are more than 100, indicating the magnetization should be stable for more than a decade, which is sufficient for future magnetic storage applications. Similar values of KV/kT were obtained by measuring the time dependence of H_{cr} using the AGM. It should be noted, however, that both techniques would be expected to give slightly lower values of KV/kT than the actual values. The temperature dependence of K will affect the value obtained from temperature-dependent measurements, and the insufficiently high magnetic field of the AGM will affect the time-dependent measurements.

The magnetic switching volume was extracted from KV and H_0 by assuming that $H_0 \approx (1/2)H_k = K/M_s$. The calculated switching volumes correspond to spheres of diameters $\sim$7 nm, which may reflect some particle growth or interactions within particle agglomerates [18].[1] However, these measurements are representative of a limited part of the switching field distribution because some of the annealed films may contain a superparamagnetic fraction of particles. Further investigations of the magnetic properties, including delta-M measurements to characterize interactions between particles, are underway.

IV. Conclusion

Self-assembled $[FePt]_{1-x}Au_x$ nanoparticles with a diameter of approximately 3.5 nm have been synthesized. Detailed structural and magnetic analyses of these nanoparticles have shown that the phase transition of FePt nanoparticles was promoted by the addition of gold. The ordering temperature has been reduced compared to pure FePt nanoparticles and FePtAg nanoparticles. This remarkable reduction of the annealing temperature is thought to be related to the defects and lattice strain introduced by gold and the segregation of gold upon annealing. Dynamic coercivity measurements reveal that the thermal stability factors are slightly higher than would be expected for noninteracting particles. The calculated switching volume of the annealed particles is larger than that of the as-made particles, suggesting that some particle coalescence may have occurred during annealing.

[1]The average particle size can be extracted from XRD measurements according to Scherrer's formula. For $[FePt]_{85}Au_{15}$ nanoparticles [see Fig. 4(b)], the average particle sizes are 5, 7, 8, and 9 nm for samples annealed at 350 °C, 400 °C, 450 °C, and 500 °C, respectively. This indicates some particle sintering and coalescence occurs during annealing

REFERENCES

[1] A. Cebollada, D. Weller, J. Sticht, G. R. Harp, R. F. C. Farrow, R. F. Marks, R. Savoy, and J. C. Scott, "Enhanced magneto-optical Kerr effect in spontaneously ordered FePt alloys: Quantitative agreement between theory and experiment," *Phys. Rev. B., Condens. Matter*, vol. 50, pp. 3419–3422, 1994.

[2] R. F. C. Farrow, D. Weller, R. F. Marks, M. F. Toney, A. Cebollada, and G. R. Harp, "Control of the axis of chemical ordering and magnetic anisotropy in epitaxial FePt films," *J. Appl. Phys.*, vol. 79, pp. 5967–5969, 1996.

[3] D. Weller, A. Moser, L. Folks, M. E. Best, W. Lee, M. F. Toney, M. Schwichert, J. Thiele, and M. F. Doerner, "High K_u materials approach to 100 Gbits/in^2," *IEEE Trans. Magn.*, vol. 36, pp. 10–15, Jan. 2000.

[4] D. Weller and A. Moser, "Thermal effect limits in ultrahigh-density magnetic recording," *IEEE Trans. Magn.*, vol. 35, pp. 4423–4439, Nov. 1999.

[5] C. M. Kuo and P. C. Kuo, "Magnetic properties and microstructure of FePt–Si3N4 nanocomposite thin films," *J. Appl. Phys.*, vol. 87, pp. 419–426, 2000.

[6] C. P. Luo, S. H. Liou, and D. J. Sellmyer, "FePt : Si_{O2} granular thin film for high density magnetic recording," *J. Appl. Phys.*, vol. 87, pp. 6941–6943, 2000.

[7] C. P. Luo, S. H. Liou, L. Gao, Y. Liu, and D. J. Sellmyer, "Nanostructured FePt: B2O3 thin films with perpendicular magnetic anisotropy," *Appl. Phys. Lett.*, vol. 77, pp. 2225–2227, 2000.

[8] B. Bian, K. Sato, Y. Hirotsu, and A. Makino, "Ordering of island-like FePt crystallites with orientations," *Appl. Phys. Lett.*, vol. 75, pp. 3686–3688, 1999.

[9] B. Bian, D. E. Laughlin, K. Sato, and Y. Hirotsu, "Fabrication and nanostructure of oriented FePt particles," *J. Appl. Phys.*, vol. 87, pp. 6962–6964, 2000.

[10] C. M. Kuo, P. C. Kuo, W. C. Hsu, C. T. Li, and A. C. Sun, "Effects of W and Ti on the grain size and coercivity of $Fe_{50}Pt_{50}$ thin films," *J. Magn. Magn. Mater.*, vol. 209, pp. 100–102, 2000.

[11] P. C. Kuo, Y. D. Yao, C. M. Kuo, and H. C. Wu, "Simulation of ultrathin lubricant films spreading over various carbon surfaces," *J. Appl. Phys.*, vol. 87, pp. 6164–6166, 2000.

[12] Y. Watanabe, N. Kimura, K. Hono, K. Yasuda, and T. Sakurai, "Microstructures and magnetic properties of Fe–Pt permanent magnets," *J. Magn. Magn. Mater.*, vol. 170, pp. 289–297, 1997.

[13] M. Watanabe, T. Masumoto, D. H. Ping, and K. Hono, "Microstructure and magnetic properties of FePt–Al–O granular thin films," *Appl. Phys. Lett.*, vol. 76, pp. 3971–3973, 2000.

[14] S. Sun, C. B. Murray, D. Weller, L. Folks, and A. Moser, "Monodisperse FePt nanoparticles and ferromagnetic FePt nanocrystal superlattices," *Science*, vol. 287, pp. 1989–1992, 2000.

[15] S. Kang, J. W. Harrell, and D. E. Nikles, "Reduction of the fcc to $L1_0$ ordering temperature for self-assembled FePt nanoparticles containing Ag," *Nano Lett.*, vol. 2, pp. 1033–1036, 2002.

[16] O. Kitakami, Y. Shimda, K. Oikawa, H. Daimon, and K. Fukamichi, "Low-temperature ordering of $L1_0$–CoPt thin films promoted by Sn, Pb, Sb, and Bi additives," *Appl. Phys. Lett.*, vol. 78, pp. 1104–1106, 2001.

[17] P. J. Flanders and M. P. Sharrock, "An analysis of time-dependent magnetization and coercivity and of their relationship to print-through in recording tapes," *J. Appl. Phys.*, vol. 62, pp. 2918–2928, 1987.

[18] B. D. Cullity and S. R. Stock, *Elements of X-Ray Diffraction*, 3rd ed. Reading, MA: Addison-Wesley, 1987, pp. 170–171.